DOI: 10.13009/EUCASS2023-918
Aerospace Europe Conference 2023 – 10TH EUCASS – 9TH CEAS

FLOw boiling REgimes iN microgravity Conditions Experiment (FLORENCE): REXUS-27 sounding rocket campaign

P. Eneren†, Y. T. Aksoy*, F. Mertens*, A. Vangeffelen*, C. Esposito*, J. Steelant**, M. R. Vetrano**
**KU Leuven, Department of Mechanical Engineering, Division of Applied Mechanics and Energy Conversion (TME), Heat and Mass Transfer group, B-3001 Leuven*
***ESA, Flight Vehicles and Aerothermodynamics Engineering Section (TEC-MPA), ESTEC, NL-2200 Noordwijk*
pinar.eneren@kuleuven.be

Abstract
Effective cooling through boiling heat transfer plays a critical role in thermal management systems for space applications. Due to the complexities of the involved phenomena, there is still a need to validate numerical models in microgravity by experimental data. Therefore, we aim to investigate the feasibility of performing low-budget and miniaturized flow boiling experiments in microgravity conditions. This communication focuses on the design and qualification of the FLORENCE experiment conducted aboard the REXUS-27 sounding rocket in November 2022. We observe increased bubble size due to coalescence in reduced gravity. This research contributes to understanding flow boiling in reduced gravity and its potential for future sounding rocket missions.

1. Introduction

Thermal management is continuously attracting interest from micro/nanoelectronics (high power density within limited physical dimensions) to aerospace (absence of buoyancy and need for heat recovery) and nuclear plants (cooling of reactors). Therefore, flow boiling represents one of the most efficient ways to transfer heat from hot spots. Although flow boiling is exploited in many engineering fields and is of great interest in space applications, it has not been fully explored in reduced gravity as a result of the additional complexities arising from the fluid flow. More specifically, space missions are becoming increasingly longer and more complex, necessitating efficient thermal control systems (TCS) to enhance performance and reduce weight and power requirements. While single-phase TCS technologies rely solely on the sensible heat of the chosen liquid, two-phase thermal management systems harness both the fluid's sensible heat and latent heat. As a result, two-phase systems exhibit a significant improvement in thermal performance [1]. These two-phase TCS technologies find widespread application, particularly in controlling propulsion system temperatures, such as those found in rocket engines.

Two-phase TCS technologies can manifest in two different forms: pool boiling and flow boiling, as illustrated in Figure 1. In pool boiling, the bulk fluid remains stationary, whereas in flow boiling, an external source, such as a pump, moves the bulk fluid over the heated surface. Pool boiling has proven to be inefficient in space applications due to the absence of buoyancy force in microgravity [1,2]. In microgravity, when a liquid-filled reservoir is placed on a heated surface, bubbles form at the interface and remain stationary. This leads to the creation of a vapor layer that insulates the surface from the liquid. Consequently, the surface temperature rises, causing vapor expansion and posing a risk of burnout. To prevent this, flow boiling is applied to remove bubbles and maintain liquid contact with the heated surface.

The understanding, prediction, and control of flow boiling in reduced gravity are strongly hampered by the absence of validated mechanistic and numerical models. Hence, creating reliable and accurate experimental databases is essential to assess the accuracy of the model predictions. To study the effect of reduced gravity on flow boiling, there are various platforms: drop towers, parabolic flights, sounding rockets, and space stations.

DOI: 10.13009/EUCASS2023-918

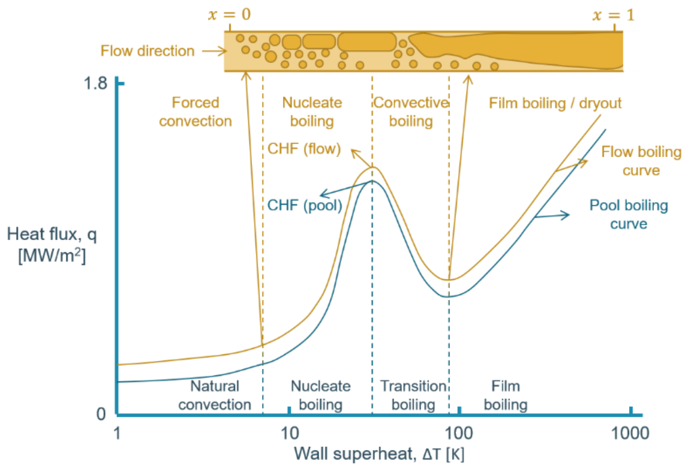

Figure 1: Comparison of the pool and flow boiling phenomena for water at 1 atm on ground [3].

Ma and Chung [4] perform microgravity experiments in a drop tower. They use FC-72 as the working fluid and a platinum wire as a heater to generate bubbles and simultaneously measure the heater's mean temperature. Via camera visualization at 30 fps, they observe that microgravity causes a notable reduction in the critical heat flux (CHF). Increasing the flow rate results in higher CHF values, and the boiling curves shift upwards in Earth's gravity and microgravity environments. Another drop tower study reports that low-speed flow boiling acts as pool boiling indicating that the CHF under microgravity is about 78–92% of that in Earth's gravity [5]. Furthermore, Liu et al. [6] observe a difference in bubble behavior between the two gravity conditions becoming more pronounced with an increase in heater length. In Earth's gravity, the channel's larger height helps prevent bubble accumulation downstream of the heated surface due to the capillary length being smaller than the channel height. In contrast, in microgravity, bubbles tend to slide on the surface, yielding a significant bubble coalescence [7], and the increased capillary length, i.e., a characteristic size below which bubbles are typically spherical, in microgravity reduces the impact of channel height on the CHF.

Baltis et al. [8] investigate flow boiling in reduced gravity during parabolic flights aboard the Novespace Airbus A300 ZeroG. For their study, FC-72 is used as the working fluid inside the tubes with 2, 4, and 6 mm diameters. Their results reveal that the flow boiling heat transfer rate in reduced gravity can exhibit two different behaviors in subcooled regime when the flow pattern is classified as bubbly flow. That is, depending on the local conditions of turbulence or vapor clot size, the heat transfer rate can either increase (up to 20%) or decrease (down to 35%). The increase in heat transfer rate is believed to be linked to increased local turbulence caused by larger bubble sizes in reduced gravity. Additionally, the different flow patterns observed at the two gravity levels may also contribute to these variations in heat transfer rate. Narcy et al. [9] perform forced convective boiling experiments with HFE-7000 under Earth's gravity and microgravity conditions during parabolic flights to measure pressure drops, void fraction, and wall temperatures. Their study shows that the transition from slug to annular flow occurs at lower flow qualities in microgravity compared to Earth's gravity. Zhang et al. [10] investigate the CHF during flow boiling using FC-72 through parabolic flight experiments aboard NASA's KC-135 turbojet. In microgravity, the phenomenon of bubble detachment is not observed. Instead, bubbles quickly merge and form relatively large vapor patches gliding along the heated wall. This behavior is consistent across all flow velocities. Based on their findings, the CHF observed in microgravity at low velocities is considerably lower than in horizontal flow in Earth's gravity. However, at higher velocities, the CHF values in microgravity start to approach those observed in Earth's gravity. This suggests that flow boiling systems would reach only optimal thermal efficiency for space applications when operating at sufficiently high velocities.

Complex geometries promote enhancement according to recent sounding rocket experiments of the flow boiling of cryogenic nitrogen [11,12]. It is essential to underline that two experimental studies has occupied the entire JAXA’s sounding rocket S-310-43 (7 m in length and 310 mm in diameter). To the best of the authors' knowledge, no other sounding rocket breadboards have been designed to investigate flow boiling. Hence, in this study, we discuss the extensive design of the FLORENCE experiment to characterize the bubbly flow and understand the flow boiling phenomenon in reduced gravity via the REXUS program. This flight platform imposes directly onto the experimental setup to ascertain certain space-proof restrictions and geometrical constraints.

DOI: 10.13009/EUCASS2023-918

1.1 REXUS: Rocket EXperiments for University Students

The REXUS/BEXUS program enables students from universities and higher education colleges throughout Europe to carry out scientific and technological experiments using research rockets and balloons. The program is implemented through a bilateral Agency Agreement between the German Aerospace Center (DLR) and the Swedish National Space Agency (SNSA). Through collaboration with the European Space Agency (ESA), the Swedish payload share is made accessible to students from other European countries. Campaign management and launch vehicle operations are handled by EuroLaunch, a cooperation between the Swedish Space Corporation (SSC) and the Mobile Rocket Base (MORABA) of DLR. Technical support throughout the project is provided by experts from DLR, SSC, ZARM, and ESA to assist the student teams. SSC's Esrange Space Center in northern Sweden serves as the launch site for both the REXUS and BEXUS missions.

REXUS experiments are conducted using a spin-stabilized rocket powered by an Improved Orion Motor. The rocket is equipped with 290 kg of solid propellant and can carry 40 kg of experiment modules to an altitude of approximately 90 km, providing around 3 minutes of spaceflight. The vehicle has a length of about 5.6 m and a body diameter of 35.6 cm. Figure 2 illustrates an example of an integrated REXUS rocket.

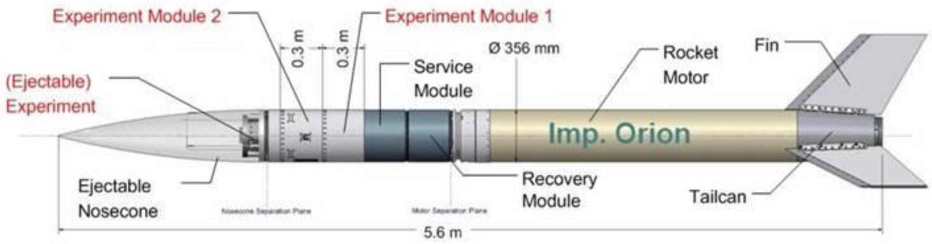

Figure 2: The schematic of a REXUS rocket [13].

To meet the rigorous demands of the REXUS program [13], the participating agencies arrange multiple technical meetings with the student teams. The aim of these meetings is to ensure that the experiments adhere to all necessary electrical and mechanical interface specifications, comply with safety regulations, and are capable of collecting valuable scientific data during the flight. During these events, the teams must demonstrate the suitability and safety of their experiments through testing, simulation, and the timely submission of comprehensive documentation. By effectively presenting their work to the experts, the teams strive to gain approval for their experiments to be included in the flight. These technical events for cycle 12 where REXUS-27 (see Figure 3) and REXUS-28 rockets were involved:

- Selection workshop at ESA - Noordwijk/The Netherlands
- Preliminary Design Review (PDR) at DLR - Oberpfaffenhofen/Germany
- Critical Design Review (CDR) at DLR - Oberpfaffenhofen/Germany
- Integration Progress Review (IPR) at KU Leuven - Leuven/Belgium
- Experiment Acceptance Review (EAR) at KU Leuven - Leuven/Belgium
- Integration Week (ITW) including vibration tests at ZARM - Bremen/Germany
- Bench test at DLR - Oberpfaffenhofen/Germany
- Spin & Balance test at DLR – Oberpfaffenhofen/Germany
- Launch campaign at ESRANGE – Kiruna/Sweden

DOI: 10.13009/EUCASS2023-918

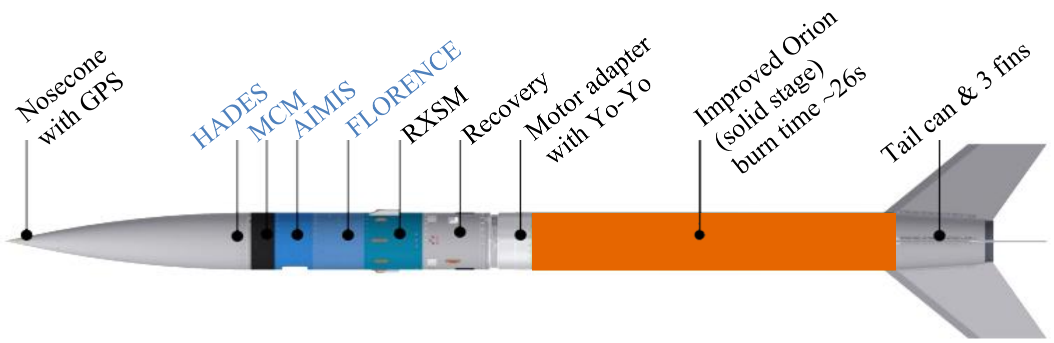

Figure 3: The schematic of REXUS-27 that successfully took off on November 5th, 2022 with a flight apogee of 84.9 km, illustrating the experiment modules in blue.

2. Design

The component selection is determined by the constraints on the maximum allowed volume, mass, and power consumption and by the durability requirements at the launch. For instance, using a preheater and an accumulator was not feasible due to the restricted power and volume. Furthermore, shortened test section length and the camera's minimum shutter time influenced the observable boiling regimes. In addition, because of the partial vacuum, convective cooling mechanisms could not be relied on to cool the working fluid downstream of the test section, and the heat exchanger was designed accordingly. Besides, the idea of a pressurized vessel and open fluidic loop was abandoned due to the extra complexity and the presence of a partial vacuum, respectively. The main components of the FLORENCE experiment are listed below.

- Working fluid (HFE-7000 from 3M, boiling point of 34°C at 1 bar, dielectric, non-flammable, non-toxic) circulated in a closed fluidic loop.
- Resistive heater (7x40 mm^2 customized from Captec).
- FESTO connectors for the fluidic loop.
- Pump (Series GA-X21 micropump) with an internal tachometer for the flow rate measurements when calibrated.
- High-speed camera (JAI SP-5000M-USB-C, 350 fps) equipped with an objective lens (Schneider Kreuznach 2/3'' MP).
- LED panel (SmartArray L6 from Lumitronix).
- T-type thermocouples (x4, from Omega).
- Absolute pressure sensor (PXM309- from Omega, range of 0 to 3.5 bar).
- Flight computer for fully autonomous system (compactRIO 9054 (c-RIO) from National Instruments).
- I/O modules (NI modules from National Instruments) NI 9211, NI 9381, NI 9485, and NI 9401.
- Customized Printed Circuit Board (PCB).
- Customized passive Heat Exchanger (HEX) with Phase Change Material (PCM, RT18HC from RubiTherm with melting temperature of 18°C).

2.1 Mechanical design

As the longitudinal acceleration can reach up to 20 g during the REXUS launch and the centrifugal forces are present due to the rocket spin (3-4 Hz), each component must be thoroughly chosen and fixed. Besides, the Center of Gravity (CoG) of the experiment module shall be located within 20 mm around the longitudinal axis. It should be noted that the total apogee of the rocket is highly affected by the payload mass. To achieve the best possible performance, it is essential to minimize the mass of the experiment modules. By keeping the module mass to a minimum, the rocket can optimize its trajectory and reach a higher apogee, i.e., longer reduced gravity.

The mechanical design baseline specifies that the outer structure consists of cylindrical aluminum modules supplied by ZARM. The modules are made of EN AW 7020-T6 aluminum and have a blue anodization finish. These modules have a diameter of 14 inches (355.6 mm) and a thickness of 4 mm. The length of the modules can vary between 120 mm, 220 mm, or 300 mm, depending on the specific configuration needed. Due to the flange interface, the entire length of the module cannot be utilized for the experiment. That is, the experiment volume allowance starts 20 mm below the top of the module to avoid any mechanical interference between experiments and any protrusion of the connectors into this space, allowing for smooth assembly. For the assembly of scientific payloads, a standard EuroLaunch D-Sub

DOI: 10.13009/EUCASS2023-918

Bracket is mounted in each experiment, above and below which adequate space should be left to facilitate the passage and mounting of cables on the walls. Plus, a section of the bulkhead should remain open to accommodate the feed-through of up to four D-SUB 15 connectors.

For 3D modelling of the FLORENCE module, as displayed in Figure 4, Fusion 360 software was used. The software also allows the calculation of CoG if the density/mass of each component is entered. Consequently, a deviation of 11.8 mm from the longitudinal axis was obtained without the outer structure and connectors. Nevertheless, it reduced to 6.7 mm owing to the bulky outer structure, thus meeting the REXUS' aforementioned requirements. The manufactured module can be seen in Figure 5.

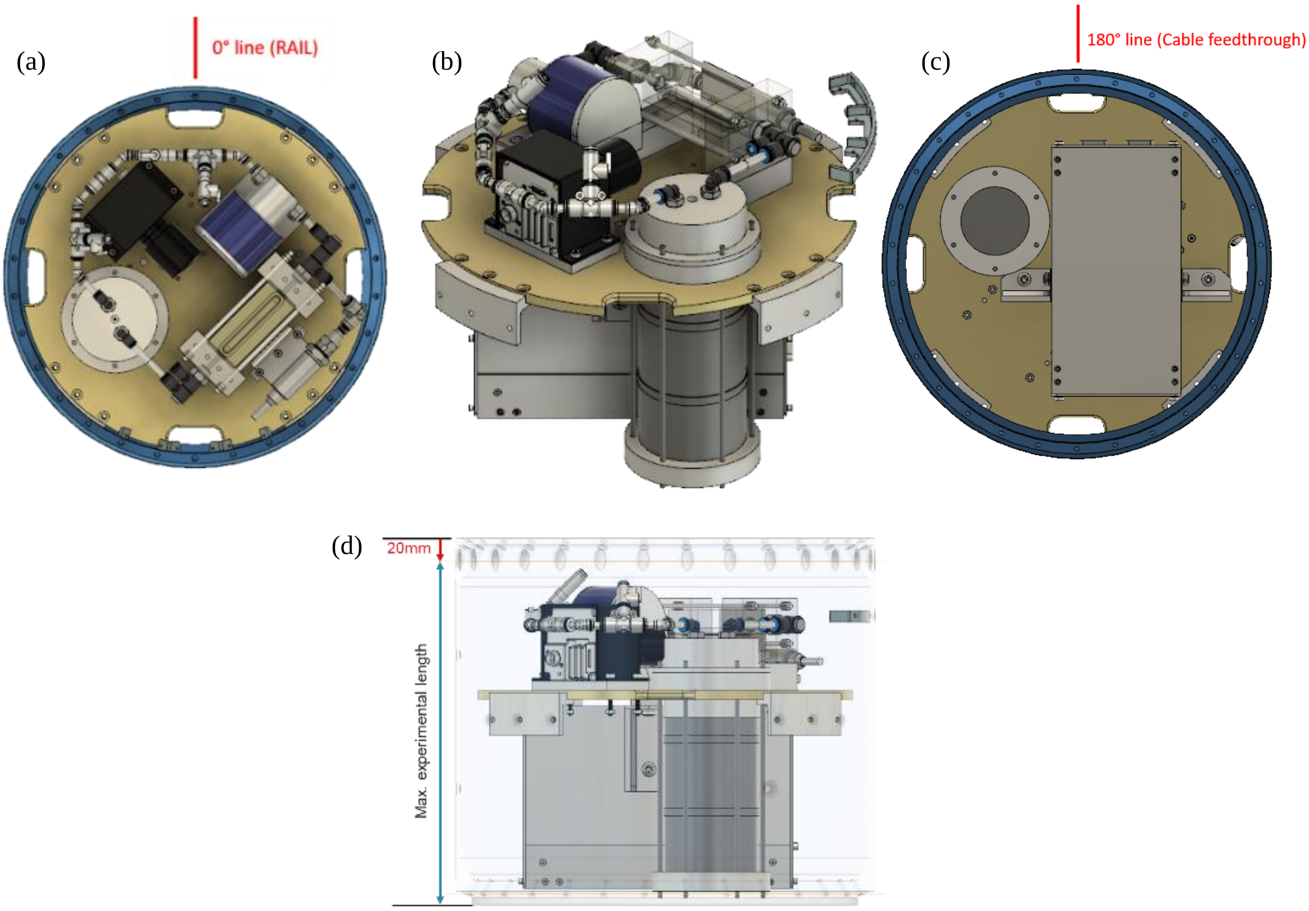

Figure 4: FLORENCE CAD design of the 300-mm length module: top view (a), oblique view (b), bottom view (c), and side view, including the height constraints (d).

Figure 5: FLORENCE experiment module (left) and the integrated REXUS-27 rocket (right).

DOI: 10.13009/EUCASS2023-918

The CHF of HFE-7000 is 18 W/cm2 when boiling occurs from a horizontal platinum wire with a diameter of 0.5 mm in a saturated quiescent fluid. However, the CHF value changes in flow boiling for various hydraulic and thermal conditions, such as mass flux and subcooling level. In our case, the flow boiling occurs inside a 82-mm long channel with a 5x5 mm^2 cross-section, i.e., a hydraulic diameter of 5 mm. A customized 7x40 mm^2 heater (one side in copper, the other is insulated with Kapton film), with a thickness of 0.2 mm and an electrical resistance of 40 Ω, is placed at the bottom of the channel. The test section is made of plexiglass material, as illustrated in Figure 6.

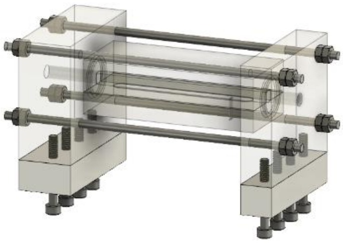

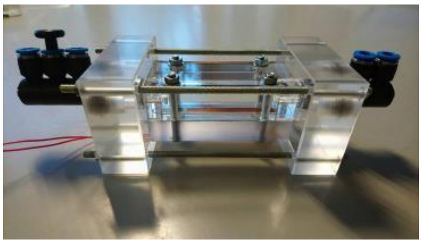

Figure 6: Test section: CAD drawing (left) and manufactured (right) with fluidic connectors.

2.2 Thermal design

Some parts of the outer structure of the REXUS rocket can experience temperatures up to 110°C (~50 seconds after lift-off), whereas, during the re-entry phase, peak skin temperatures exceeding 200°C are anticipated. These elevated temperatures are conducted to internal components, including the bulkheads. Therefore, proper insulation was foreseen for the design of the experiment. For instance, to minimize heat conduction, a minimum insulation buffer of 10 mm made of Teflon was provided for each component from the bulkhead. Since the working fluid is heated to observe the boiling phenomenon, the fluid has to be cooled down so that the fluid temperature at the inlet of the test section is kept constant (see Figure 7).

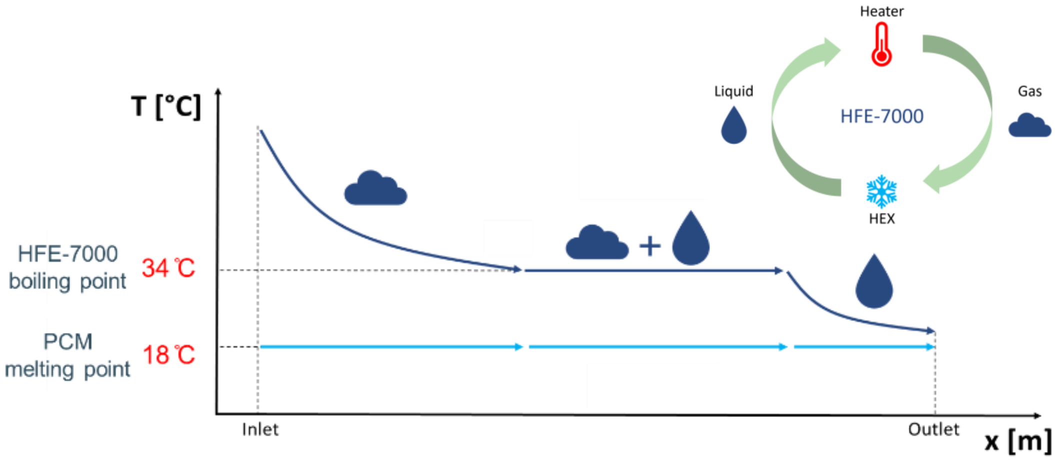

Figure 7: FLORENCE HEX design in terms of passive cooling.

Due to REXUS power limitations, a passive cooling method via Phase Change Material (PCM) was applied by considering the following factors: the melting temperature of the PCM should be lower than the boiling temperature of the working fluid, and the PCM should possess a large latent heat to minimize its mass. Consequently, RT18HC from RubiTherm was chosen, with a melting temperature of 18°C and a latent heat of 260 kJ/kg. The PCM was placed inside a 500 ml thermos Dewar Flask (GSS 500 from KGW Isotherm). Inside the thermos, a serpentine copper pipe was inserted to allow the flow of hot working fluid. Then, the fluid was cooled by exchanging heat with the PCM. To address the low thermal conductivity of the PCM, a copper mesh was also added to the thermos, whose lid is thermally insulated. The HEX design can be seen in Figure 8. It should be noted that the temperature of the working fluid would rapidly increase after the PCM is fully melted. Hence, for optimal experimental conditions, it is necessary to maintain the PCM temperature around its melting point.

DOI: 10.13009/EUCASS2023-918

Figure 8: FLORENCE HEX design including a vacuum-insulated thermos, a copper serpentine, an aluminum lid, a thermocouple feedthrough, and a copper mesh.

2.3 Electrical design

The REXUS Service Module (RXSM) functions as a means of communication between the onboard systems/experiments and the ground station(s). Each experiment is assigned a standardized RXSM interface via D-SUB 15 connector, which incorporates all power delivery, experiment control, and bidirectional data exchange (TeleMetry/TeleCommand TM/TC). The feed-through harness, responsible for linking the experiments to the service system, is designed and supplied by ZARM. The RXSM is responsible for providing power at a standard 28 V DC. The supply voltage can range from 24 V to 36 V, depending on the state of the onboard batteries. The experiment needs to be capable of handling voltage variations that may occur when transitioning the RXSM from external (regulated) power to internal (battery) power. During this switching process, the peak power consumption should not exceed 3 A per experiment line, whereas the average power consumption should stay below 1 A mean. Therefore, each experiment typically receives ~28 W. The experiment power is switched off before landing for safety reasons (~T+600 s). The electronic box (E-Box) houses the PCB that contains active components, providing the main connection between the c-RIO and actuators/sensors. More specifically, these components facilitate DC-DC conversions, initiate the LED, heater, pump, and the pressure sensor, and collect the temperature, pressure, and heater's current and voltage data. The global map of the FLORENCE PCB is illustrated in Figure 9.

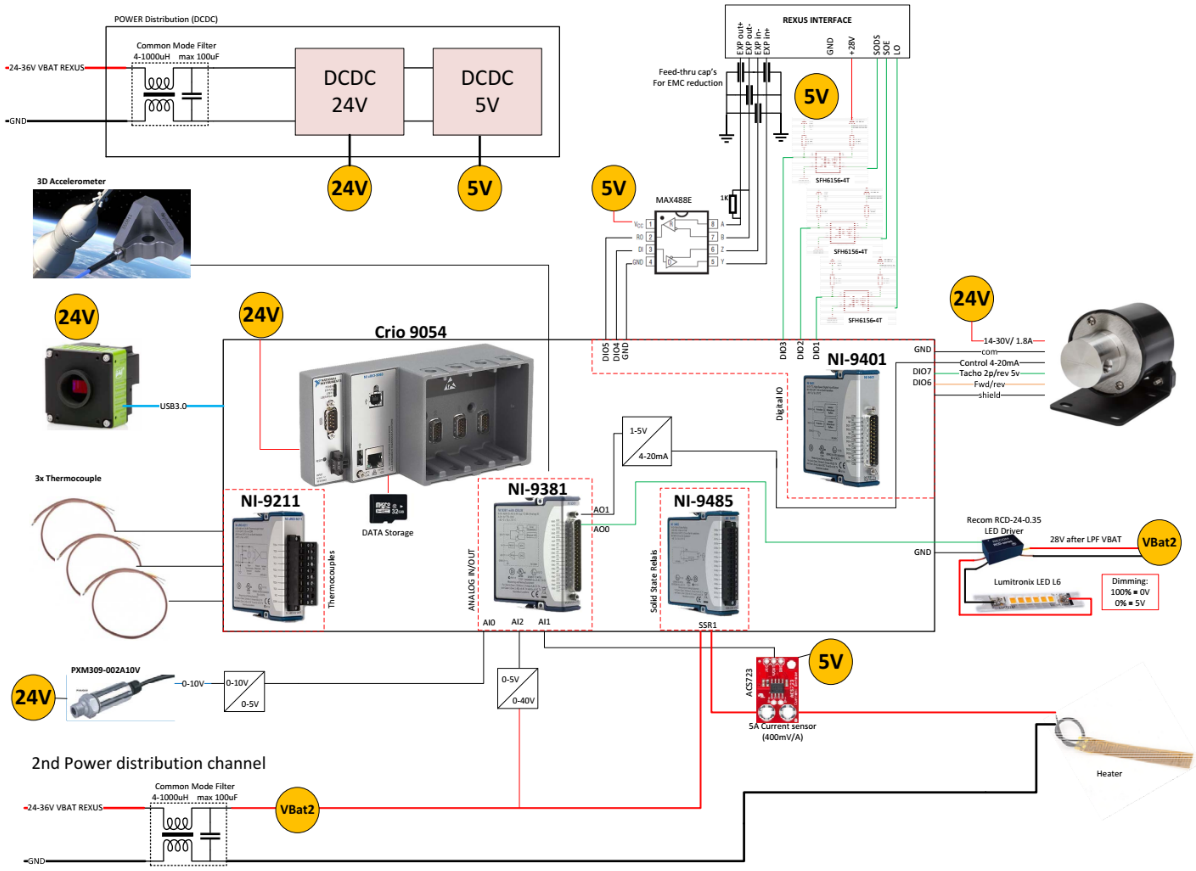

Figure 9: FLORENCE electrical design with the global electronics map.

DOI: 10.13009/EUCASS2023-918

According to Table 1, with a total power consumption of 40.6 W, the FLORENCE module exceeds 28 W, which requires the use of an extra power line. The power consumption for all sensors (e.g., camera and pressure sensor) and control electronics (e.g., c-RIO and the PCB) are considered in the IDLE mode.

Table 1: Power consumption of the FLORENCE module.

	Voltage [V]	**Current [A]**	**Power [W]**
IDLE	28	0.52	14.6
LED	28	0.69	19.3
Pump	28	0.58	16.2
Pump + Heater	28	1.28	35.8
Pump + LED	28	0.75	21.0
Pump + LED + Heater	28	1.45	**40.6** (Total)

The local ground of the PCB was connected to the E-Box, which was securely fastened to the bulkhead in an electrically conducting way. The housing of the E-Box was constructed from aluminum to possess electrical conductivity and equipped with a suitable screw connection and electrical feedthroughs. Additionally, a shielding effectiveness of at least 20 dB was attained to effectively contain undesired emissions within the housing and prevent external radiation from the outside.

2.4 Software design

The RXSM provides 3 separate control lines for each experiment module. The Start of Data Storage (SODS) and the Start/Stop of the Experiment (SOE) can be activated either through a timeline or by the EGSE (Electrical Ground Support Equipment) system using an umbilical connection. Lift-Off (LO) is triggered when the umbilical connector is detached from the RXSM as the rocket departs from the launcher. Finally, all timeline events are synchronized and correlated with the physical LO signal (T+0 s).

Both short and long drops in the telemetry connection must be considered when developing the software. Moreover, data losses are anticipated during the launch and the re-entry phase. However, the bit error rate is less than 10^{-6} bit for the rest of the flight. Several tests were performed using simulated dropouts in the Service System Simulator to ensure the experiment's capability to handle potential telemetry issues.

The commands are transmitted to the experiments using the TX-lines of an RS-422 channel. Similarly, for the transfer of experiment data to the RXSM, the RS-422 interface is utilized. The standard baud rate is 38.4 kbit/s, with a format comprising 8 bits, 1 start and stop bit and no parity. The experiment teams are responsible for data formatting, failure detection, and correction. The baud rate was limited to 30 kbit/s (~80%) of the maximum data throughput to prevent channel bandwidth overload. Similarly, to avoid buffer overflows in the RXSM-TM system packets with a maximum size of 64 bytes were constructed.

The FLORENCE software architecture, demonstrated in Figure 10, mainly consists of a ground station and an autonomous working module. The ground station enables the user to control various actuators, such as the pump, LED, and heater, until the SODS signal is received. It also facilitates the monitoring of sensor data while the system remains powered. This includes temperature measurements of the inlet, outlet, PCM, and heater, as well as readings for inlet pressure, pump rotation speed, camera status, and heater current and voltage. Upon receiving the SODS, all the actuators are simultaneously initiated, while the sensor data are recorded to guarantee synchronization across the entire system. The SODS is received 120 s before the LO signal, which starts the recording of the ground conditions as a reference, as well as hyper and reduced gravity. To prioritize data security, the system automatically shuts down after 300 s once all the data are saved on the internal memory of the c-RIO and the SD card.

DOI: 10.13009/EUCASS2023-918

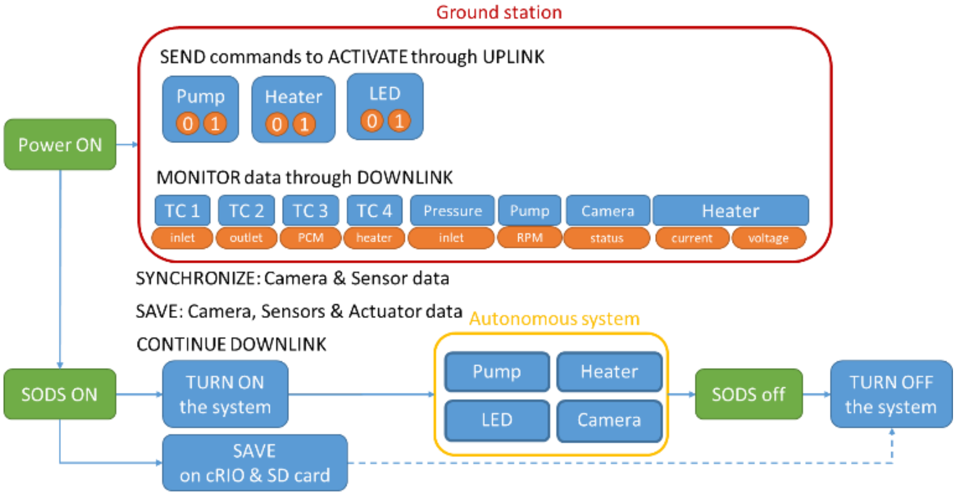

Figure 10: FLORENCE software architecture with the REXUS signals.

3. Experiment Verification

Environmental tests were conducted to validate the proper functioning of the experiments under the most extreme conditions that could be encountered during the countdown, launch, and flight to simulate worst-case scenarios.

3.1 Leakage test

Due to the circulation of HFE-7000 (> 2 ml), each fluidic component and the related subsystems were tested with pressurized air of 3 bar (x3 working pressure) immersed in a bucket of water. First, component tests were performed on FESTO components. Then, subsystem tests were carried out on the pump + FESTO components, test section + FESTO components, HEX thermos + FESTO components, and HEX serpentine + FESTO components.

3.2 Vacuum test

The vacuum test is required to assess the performance of not only experiments intended for vacuum conditions but also to guarantee the proper functioning of electrical components in the absence of convective cooling. Hence, the FLORENCE experiment was placed inside a vacuum chamber with a pressure of ~100 mbar, and several thermocouples were attached to the components, i.e., camera, PCB, and c-RIO. The experiment was operated while the pressure in the vacuum chamber was gradually reduced, and all experiment data were recorded throughout the test. The module was kept in a similar condition to that of the actual ascent of the flight. After the functional test and flight sequence were completed, the experiment continued for an additional 15 minutes to detect any potential leaks or overheating issues. As can be deduced from Figure 11, nominal performances of the electronic components were observed, and acceptable temperature increases of the electronics were obtained at the end of the vacuum test.

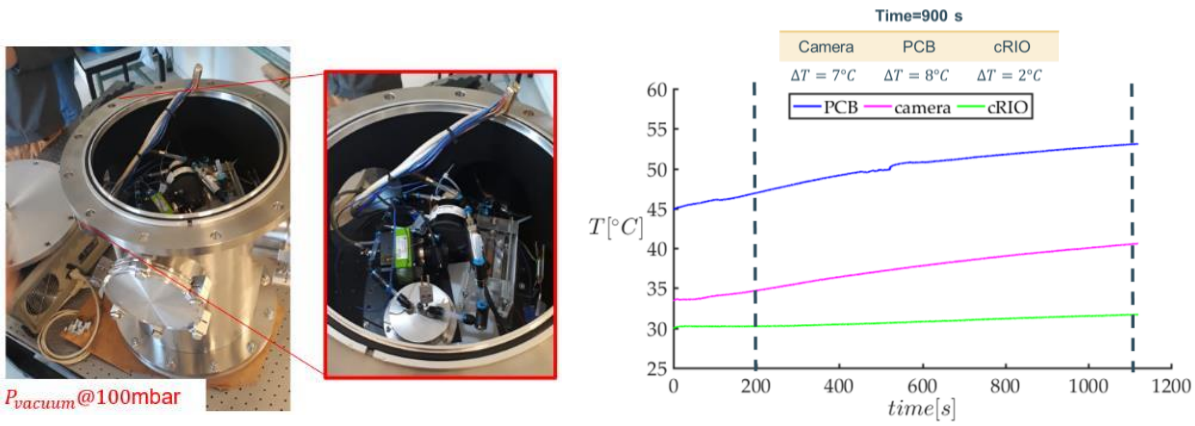

Figure 11: Vacuum testing of FLORENCE module.

DOI: 10.13009/EUCASS2023-918

3.3 Vibration test

For REXUS missions, it is standard practice to perform acceptance level tests on all experiments. By subjecting each experiment to vibration testing, its ability to resist the mechanical stresses of the launch is verified, ensuring its resilience and reliability during the mission. These tests are performed to see whether an experiment has the potential to impact the other scientific payloads or the flight dynamics of the whole rocket. After the experiment was securely mounted on a vibration table using an appropriate fixture, critical components were equipped with accelerometers to track their response curves, as indicated in Figure 12. Following each axis of vibration, functional tests and inspections were conducted. Then, vibration was applied in the X, Y, and Z axes according to the specifications for the Improved Orion vehicle. Before and after each load-vibration test, a resonance search run was performed at a low level (0.25 g, 5 - 2000 Hz, 2 octaves/min) to identify the Eigenfrequencies of the test items. Each random load test took 20 s per axis.

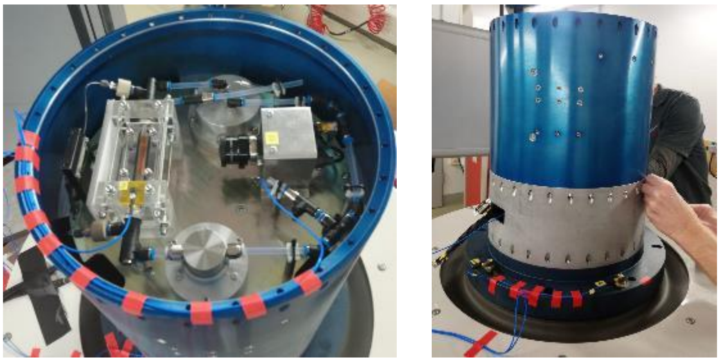

Figure 12: Vibration tests performed on the FLORENCE module during Integration Week (ITW) at ZARM.

4. Results

The comparison of the flow boiling phenomenon on the ground and on the REXUS-27 sounding rocket under reduced gravity (0.0589 g) can be seen in Figure 13, where the bubble dynamics drastically change due to the absence of gravity. The bubble coalescence leads to the formation of larger bubbles, and as they grow in size, their attachment to the heater becomes stronger, increasing the resistance to their detachment.

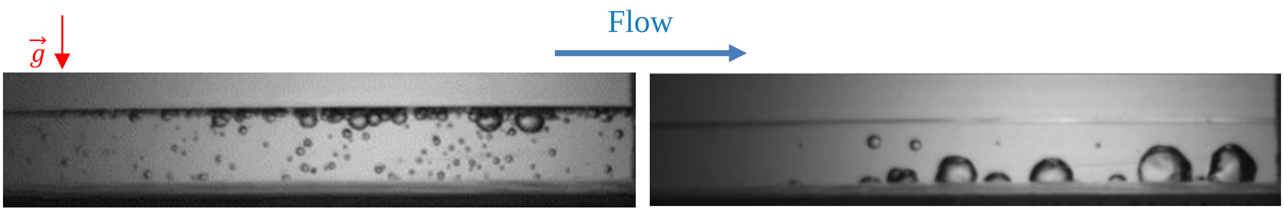

Figure 13: Flow boiling experiment: on the ground (left), on REXUS-27 sounding rocket under reduced gravity (right).

The post-processing of the camera raw images (recorded at 350 fps) comprises a simplified bubble detection algorithm, such as background subtraction, binarization, and circle detection. Figure 14 depicts the bubble evolution based on the corresponding bubble equivalent area. Due to the buoyancy force on Earth's gravity, the bubbles detach quickly without coalescence. The time axis for Earth's gravity goes up to 0.009s, whereas the axis for the reduced gravity goes up to 0.45 s as the bubbles detach from the surface at least 1 order of magnitude slower in the absence of gravity. Although the bubble growth rate under Earth's gravity is unclear due to a lack of sufficient data points, it is clear that the bubbles become significantly larger under reduced gravity.

DOI: 10.13009/EUCASS2023-918

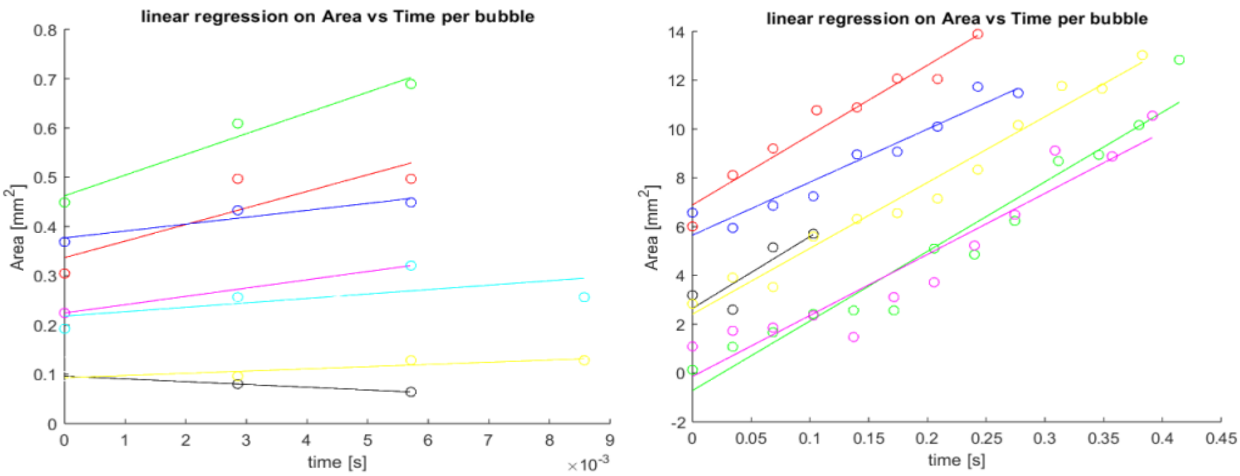

Figure 14: Bubble growth evolution: on ground (left), on REXUS-27 sounding rocket under reduced gravity (right). Each bubble is represented by a different color.

5. Conclusion

In this communication, we present the design and the qualification of the FLOw boiling REgimes iN microgravity Conditions Experiment (FLORENCE), launched on board the REXUS-27 sounding rocket in November 2022. In reduced gravity, we observe larger bubbles forming as a result of their coalescence and we are currently working on the correlation of the sensor data to the bubble dynamics.

A REXUS experiment module, despite its lower cost, can gather valuable data that can only be surpassed by a significantly more expensive commercial sounding rocket with longer durations of reduced gravity and by the experiments performed on the International Space Station (ISS) for extended periods. The development of a lightweight, low-cost, and compact flow boiling module for the REXUS missions offers a valuable platform for scientific research, particularly for projects with budget constraints, and contributes to the advancement of knowledge in the field of flow boiling in reduced gravity.

Acknowledgements

We would like to express our sincere appreciation to our technicians, Hans Van Eyken, Tom Henskens, Thomas Pilkington, Eddy Smets, and Gunther Penninckx for their invaluable contributions to the manufacturing process. We also gratefully acknowledge the European Space Agency (ESA) and the Faculty of Engineering Science KU Leuven for having funded the research activity, and the Fonds Wetenschappelijk Onderzoek - Vlaanderen (FWO) for the travel grant (K1A1623N).

References

[1] C. Konishi, I. Mudawar, Review of flow boiling and critical heat flux in microgravity, Int. J. Heat Mass Transf. 80 (2015) 469–493. https://doi.org/10.1016/j.ijheatmasstransfer.2014.09.017.
[2] T. Oka, Y. Abe, Y. Mori, A. Nagashima, Pool Boiling Heat Transfer in Microgravity : Experiments with CFC-113 and Water Utilizing a Drop Shaft Facility, JSME Int. J. Ser. B Fluids Therm. Eng. 39 (1996) 798–807. https://doi.org/10.1299/jsmeb.39.798.
[3] M.C. Vlachou, J.S. Lioumbas, T.D. Karapantsios, Heat Transfer Enhancement in Boiling Over Modified Surfaces: a Critical Review, Interfacial Phenom. Heat Transf. 3 (2015) 341–367. https://doi.org/10.1615/interfacphenomheattransfer.2016014133.
[4] Y. Ma, J.N. Chung, An experimental study of critical heat flux (CHF) in microgravity forced-convection boiling, Int. J. Multiph. Flow. 27 (2001) 1753–1767. https://doi.org/10.1016/S0301-9322(01)00031-3.
[5] Y. Zhang, B. Liu, J. Zhao, Y. Deng, J. Wei, Experimental Study of Subcooled Flow Boiling Heat Transfer on a Smooth Surface in Short-Term Microgravity, Microgravity Sci. Technol. 30 (2018) 793–805. https://doi.org/10.1007/s12217-018-9629-2.
[6] B. Liu, B. Yuan, J. Zhou, J. Zhao, P. Di Marco, Y. Zhang, J. Wei, Y. Yang, Analysis of the critical heat flux

DOI: 10.13009/EUCASS2023-918

of subcooled flow boiling in microgravity, Exp. Therm. Fluid Sci. 120 (2021) 110238. https://doi.org/10.1016/j.expthermflusci.2020.110238.

[7] Y. Zhang, B. Liu, J. Zhao, Y. Deng, J. Wei, Experimental study of subcooled flow boiling heat transfer on micro-pin-finned surfaces in short-term microgravity, Exp. Therm. Fluid Sci. 97 (2018) 417–430. https://doi.org/10.1016/j.expthermflusci.2018.05.003.

[8] C. Baltis, G.P. Celata, M. Cumo, L. Saraceno, G. Zummo, Gravity influence on heat transfer rate in flow boiling, Microgravity Sci. Technol. 24 (2012) 203–213. https://doi.org/10.1007/s12217-012-9298-5.

[9] M. Narcy, E. de Malmazet, C. Colin, Flow boiling in tube under normal gravity and microgravity conditions, Int. J. Multiph. Flow. 60 (2014) 50–63. https://doi.org/10.1016/j.ijmultiphaseflow.2013.11.011.

[10] H. Zhang, I. Mudawar, M.M. Hasan, Flow boiling CHF in microgravity, Int. J. Heat Mass Transf. 48 (2005) 3107–3118. https://doi.org/10.1016/j.ijheatmasstransfer.2005.02.015.

[11] W. Sarae, K. Kinefuchi, D. Yabusaki, D. Sugimori, T. Fujita, K. Okita, Y. Umemura, K. Fujimoto, H. Negishi, H. Kobayashi, T. Himeno, T. Sato, S. Nonaka, Sounding Rocket Experiment on Chill-down Process with Liquid Nitrogen in a Complex Channel, 51st AIAA/SAE/ASEE Jt. Propuls. Conf. (2015). https://doi.org/10.2514/6.2015-4213.

[12] K. Kinefuchi, W. Sarae, Y. Umemura, T. Fujita, K. Okita, H. Kobayashi, S. Nonaka, T. Himeno, T. Sato, Investigation of Cryogenic Chilldown in a Complex Channel Under Low Gravity Using a Sounding Rocket, J. Spacecr. Rockets. 56 (2019). https://doi.org/10.2514/1.A34222.

[13] A. Kinnaird, Guidelines for Student Experiment Documentation, 2018. https://rexusbexus.net/wp-content/uploads/2018/11/RXBX_SED_guidelines_v6-0_23Nov18.pdf.